GEOLOGICA CARPATHICA, 42, 6, BRATISLAVA, DECEMBER 1991
315–322

DENSITY AND GEOTHERMAL MODELLING OF THE WESTERN CARPATHIAN EARTH'S CRUST

MIROSLAV BIELIK,[1] DUŠAN MAJCIN,[1] OTO FUSÁN,[1] MILOSLAV BURDA,[2] VINCENC VYSKOČIL[2] and JIŘÍ TREŠL[2]

[1] Geophysical Institute, Slovak Academy of Sciences, Dúbravská 9, 842 28 Bratislava, Czecho-Slovakia
[2] Geophysical Institute, Czecho-Slovak Academy of Sciences, Boční II, 141 31 Prague

(Manuscript received May 18, 1990; accepted in revised form June 20, 1991)

Abstract: The submitted work presents density and geothermal modelling in profiles KP-I, KP-II, KP-III and KP-IV. At the same time it deals with mathematical modelling of stress field in profile KP-III. This modelling has proved that the Carpathian gravity low results from combined effects of low-density Flysch Belt as well as Foredeep rocks, granitoids and crystalline schist complexes piled up in the northern Inner Carpathians as a result of their nappe structure. From a regional point of view, geothermal activity declines from the inner units of the Western Carpathians to the outer ones, whereas the share of Earth's crust radiogenic heat sources in the surface heat flow drops in the opposite direction. Mathematical modelling of the stress field has revealed that in the northern tract of the Inner Carpathians the field is of compressional character, whereas in the southern one the stress field is dilatational.

Key wods: Western Carpathians, density and geothermal models, lithosphere, stress field.

Introduction

In the past five years, much attention was paid to two-dimensional density and geothermal modelling of the Eart's crust along selected profiles through the Western Carpathians. Of course, these approaches could have taken place only after at least basic seismic data on the Earth's crust and/or lithosphere had been obtained. These include mainly data on velocity courses, particularly those of longitudinal and transverse waves, depth of important seismic discontinuities such as the Moho discontinuity etc. On the other hand we have to emphasize that the number of seismic-velocity profiles in the Western Carpathian area is inadequate. That is why we have decided to apply also geothermal modelling in addition to the method of gravity modelling in the investigation of the Western Carpathian deep structure and dynamics. We did so despite the fact that these approaches yield more equivocal results than seismic methods alone. Application of other geophysical and geological data, however, may make the results more reliable. The interpreted profiles are shown in Fig. 1. Attempts to mathematically model stress field in a given environment also became a significant positive feature in resolving Earth's crust dynamics. This is proved by the following works: Bott & Kusznir (1984), Turcotte & Schubert (1982), Turcotte & Oxburgh (1976), Watts et al. (1975) and others.

Our compilation of the Earth's crust models in the Western Carpathians area was based on the following geophysical and geological information: the course of the Moho discontinuity (Mayerová et al. 1985) seismic reflection profiles (Tomek et al. 1987, 1989), drillhole data (Biela 1978), gravity data (Ibrmajer 1978), density data (Eliáš & Uhmann 1968; Husák 1986; Šefara et al. 1987), surface heat frow density (Král 1987), thermal conductivity coefficient and heat generation (Král 1985; Husák 1986).

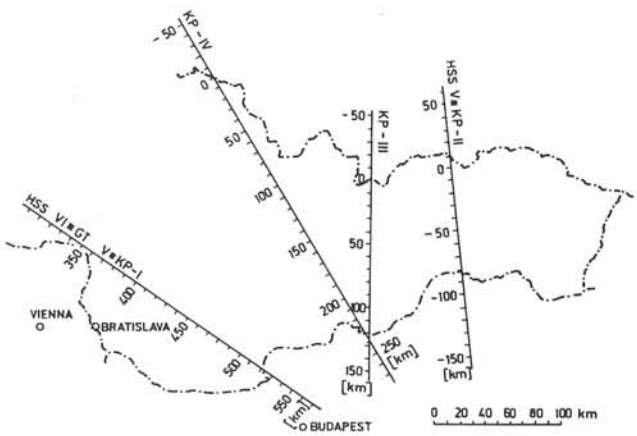

Fig. 1. Location of interpreted profiles across the Western Carpathians.

Density modelling

To calculate gravity effect of two-dimensional bodies in density modelling along profiles, we have employed Talwani's procedure (Talwani 1973), whereas anomalous bodies of

different shapes, i.e. other than two-dimensional, have been solved by Rasmussen and Pedersen's (1979) method.

The problem is dealt with in more detail by Vyskočil et al. (1990). Densities of individual bodies are related to a four--layer reference model (Bielik et al. 1987).

The evaluation of all available geological and geophysical data had made it possible to compile initial basic geologic--density models which were later gradually upgraded. The total gravity effect G_Σ of a density model (Burda et al. 1985; Bielik et al. 1987) along a profile equals to the sum of gravity effects G_1, G_2, G_3 (Figs. 4–6), G_1 being gravity effect of anomalous masses at depths of up to 10 *km*, G_2 from 10 to 25 *km* and G_3 from 25 to the lower margin of the Moho discontinuity.

Geothermal modelling

To model geothermal characteristics of temperature distribution and heat flow density, it is at first necessary to determine thermophysical parameters and then to resolve mathematic-physical problems related to heat transfer in a given environment. As already mentioned, the calculation of the geothermal models must have been based on the results of geologic-density modelling because of the lack of seismic data. The character of these initial basic data also affected the procedure of determining thermal conductivity k and heat generation f. At shallow parts of the upper Earth's crust (Blížkovský et al. 1985), both these parameters were calculated as weighted average of measured values according to petrographic composition and stratigraphic assignation of the geological structure concerned (Majcin 1989). Elsewhere in the Earth's crust and upper mantle, the parameters were derived from the analyses of their dependence on depth as well as from thermal dependence (Čermák & Bodri 1985). The magnitude of heat generation was derived from empirical relationships between heat generation and volume density (Büntebarth 1982; Rybach & Büntebarth 1982, 1984).

Heat transfer in sections was approximated by its predominant stationary component, which can be expressed by the formula

$$div\ (k.\ grad\ U) = f.$$

The rectangular area marked in Fig. 2 was outlined to meet the following conditions: at the upper margin – temperature pattern for sea level, at lateral margins – zero heat flow density in horizontal direction, and finally at the lower margin – heat flow vertical component calculated by solving inverse problem by means of iterative method. The course of heat flow density was gradually optimized to cope with the required smoothness and to minimize differences between calculated and measured values of surface heat flow density. Because of the complex distribution of thermophysical parameters, direct problems of stationary heat transfer were solved by Finite difference method, and systems of algebraic equations obtained in this manner were then treated by super relaxation method (Vazov & Forsayt 1963; Samarsky & Andreyev 1976; Samarsky & Nikolayev 1978). The non-linearity of the solved problems (resulting from taking into account thermal dependence of thermal conductivity) was supressed by iterative linearization approach.

Stress field modelling

The resulting stress field in the lithosphere comprises diverse mutually superposed sources (Bott & Kusznir 1984). One of the causes is the existence of surface topography and density inhomogeneities in the Earth's crust. The lower boundary of the elastic lithosphere is roughly defined by the isotherm $T \approx 600\ °C$, the value corresponding to the "effective" elastic thickness of 10–60 *km* (Turcotte & Schubert 1982).

To calculate the two-dimensional stress field, we employed the model of a homogeneous incompressible elastic slab

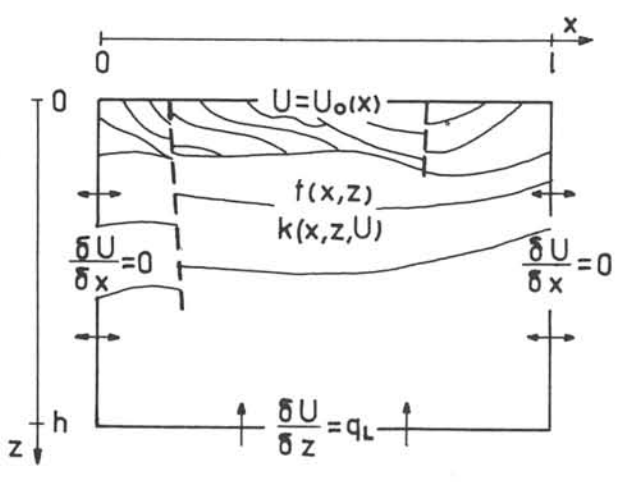

Fig. 2. Configuration of model problems with determined boundary conditions.
U – temperature field pattern, f – heat generation pattern, k – thermal conductivity, q_L – heat flow density pattern at the lower boundary of the model, U_o – temperature field pattern at the upper boundary of the model.

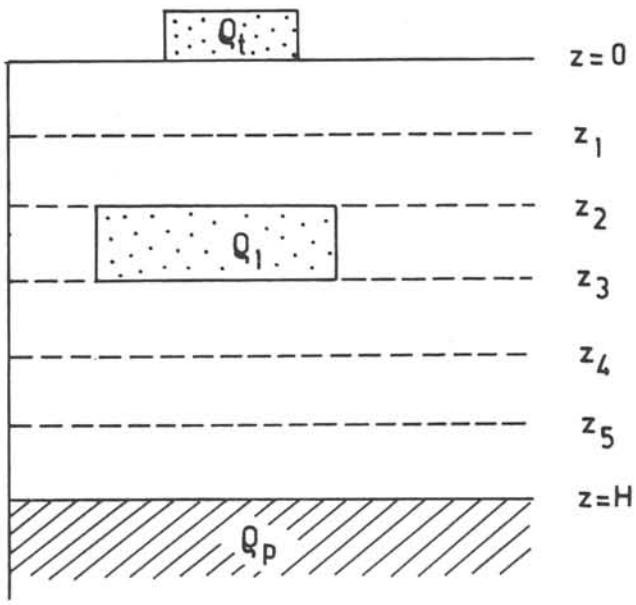

Fig. 3. Model of a homogeneous incompressible elastic slab.
ϱ_t – density of topographic masses, ϱ_1 – density inhomogeneity, ϱ_p – density of liquid substratum.

floating on liquid basement of higher density ϱ_p (Fig. 3). The sources of stress include:

a – Terrain topography of altitude h and density ϱ_t gives rise to pressure $p = \varrho_0 gh$ at the upper margin $z = 0$.

b – Density inhomogeneities $\varrho_1 = \varrho - \varrho_0$ represent body force $F = \varrho_1 g$.

The equation of static equilibrium and continuity is valid for each layer

$$-grad\ p + \mu\ \Delta^2 \vec{u} + \varrho_1 g = 0$$
$$div\ \vec{u} = 0$$

where p is pressure, $\vec{u}$ $(u,\ 0,\ w)$ displacement vector, μ elasticity coefficient, g magnitude of gravitational acceleration. If potential Ψ is defined by formulae $u = -\delta\psi/\delta z$ and $w = \delta\psi/\delta x$, the following harmonic solution relatove to x is obtained:

$$\psi(x, z) = Ae^{kz} + Be^{-kz} + Cze^{kz} + Dze^{-kz} - ig\varrho_1^0/\mu k^3)\, e^{jkx}\, p(x, z) = 2\mu k\ (Ce^{kz} + De^{-kz})\ ie^{jkx},$$

where ϱ_1^0 is amplitude of internal density inhomogeneities. Components of stress tensor result from Hook's law for incompressive environment (Eringen 1967):

$$\sigma_{xx} = -p + 2\mu\delta u/\delta x$$
$$\sigma_{zz} = -p + 2\mu\delta w/\delta z$$
$$\sigma_{xz} = \mu\ (\delta u/\delta z + \delta w/\delta x).$$

Results of modelling

The evaluation of the obtained results of the gravity and geothermal profiles indicates some interesting data on the Western Carpathian deep structure.

Figs. 4–6 show examples of gravity and geothermal models along profiles KP-II, KP-III and KP-IV. The results of the gravity and geothermal model along profile KP-I (HSS No. VI ≡ Geotraverse V) have already been published by Blížkovský et al. (1986).

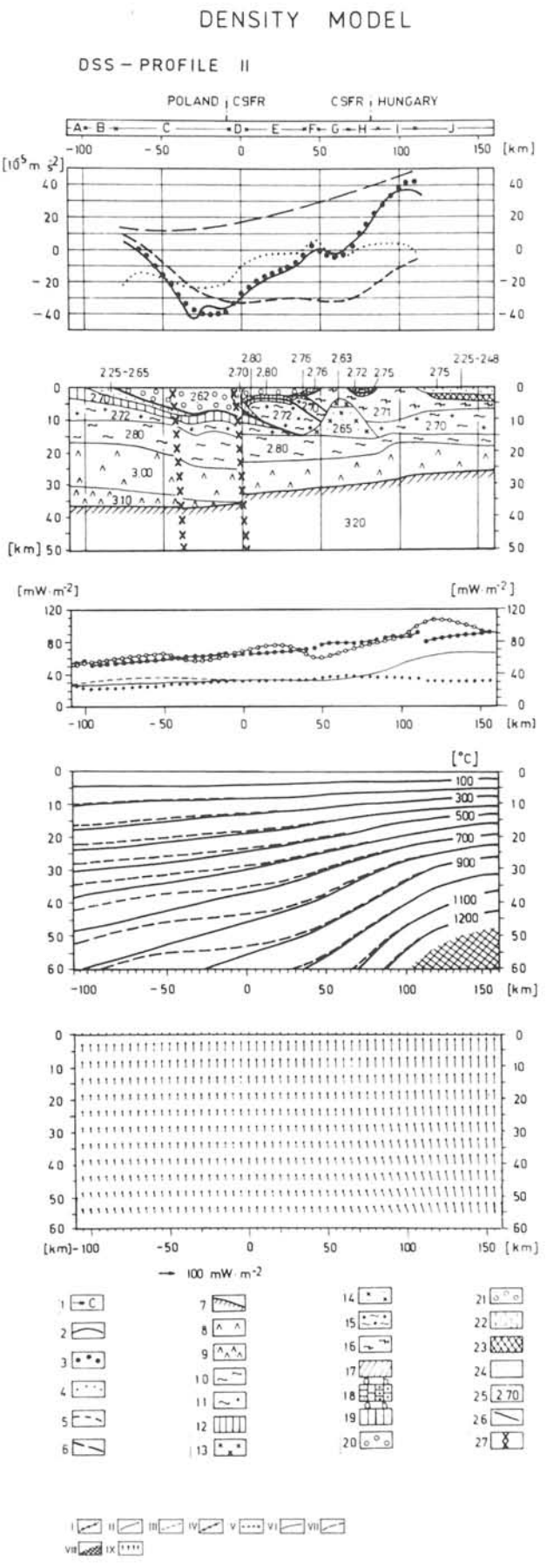

Fig. 4. Density and geothermal model of the Earth's crust along profile KP – II (HSS No. V).

Legend: 1 – boundaries of principal geological units (A – Paleozoic cover of Platform, B – Carpathian Foredeep, C – Outer Flysch Belt, D – Klippen Belt, E – Inner Carpathian Paleogene, F – Galmus Mesozoic, G – Volovské vrchy Paleozoic, H – Slovak karst Mesozoic, I – Szendrö Paleozoic, J – Pannonian Basin); 2 – Bouguer anomaly values; 3 – total gravity effect; 4 – gravity effect of contrast masses at depths of up to 10 *km*; 5 – gravity effect of contrast masses at depths of 10–25 *km*; 6 – gravity effect of contrast masses at depths of 25–40 *km*; 7 – section of Moho discontinuity; 8–9 – lower crust; 10 – lower part of upper crust; 11 – crystalline schists, granitoids whose density is 2.70/2.72 Mgm^{-3}; 12 – Paleozoic cover of Platform; 13 – Alpine granites; 14 – granodiorites; 15 – Tatric (Veporic) crystalline schists, granitoids whose density is 2.72 Mgm^{-3} (2.70 Mgm^{-3}); 16 – Paleozoic; 17 – envelope Mesozoic of Veporicum; 18 – Mesozoic (a – Galmus, b – Slovak karst); 19 – Mesozoic (a – Tatric, b – Krížna Nappe); 20 – Outer Carpathian Paleogene; 21 – Inner Carpathian Paleogene; 22 – Klippen Belt; 23 – Hungarian Midmountains Mesozoic; 24 – Pannonian Basin Neogene; 25 – rock density in Mgm^{-3}; 26 – thrust lines; 27 – deep-seated fault.

I–IX see legend to Fig. 6 (profile KP-II).

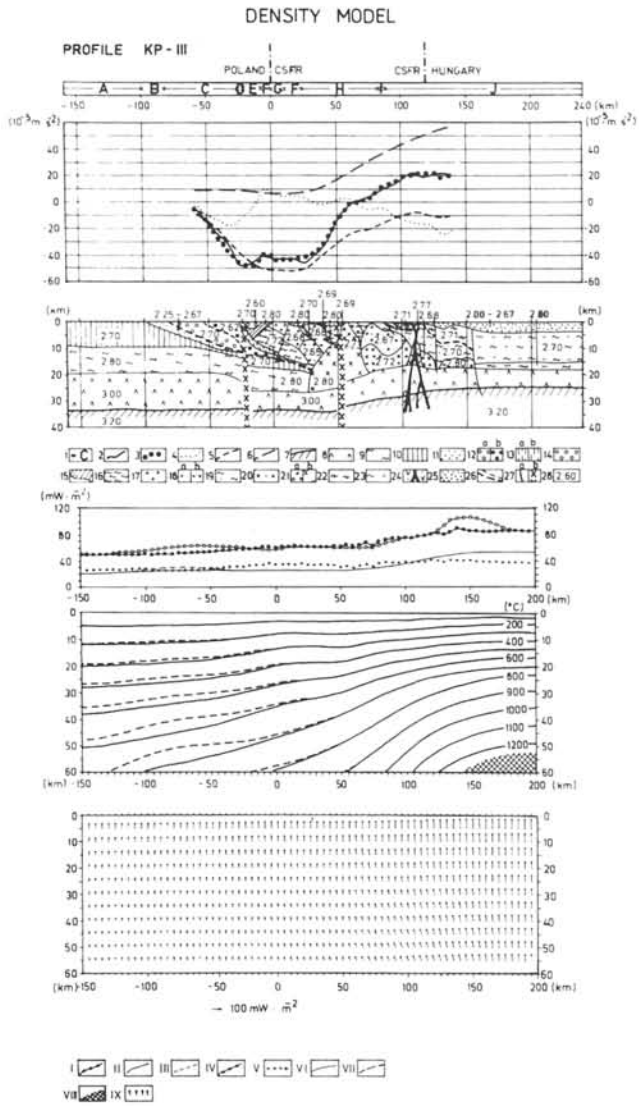

Fig. 5. Density and geothermal model of Earth's crust in profile KP-III.

Legend: 1 – boundaries of geological units A – Platform, B – Carpathians Foredeep, C – Flysch Belt, D – Klippen Belt, E – Inner Carpathian Paleogene, F – Inner Carpathian Mesozoic (envelope series, Krížna and Choč Nappes), G – Tatricum, H – Veporicum, I – Gemericum, J – Neogene; 2–7 – see explanations to Fig. 4 (profile KP-II); 8 – lower crust; 9 – lower part of upper crust; 10 – Platform Paleozoic and crystalline; 11 – Foredeep; 12 – Flysch Belt (a – Silesian Nappe, b – Magura Nappe); 13 – a) Klippen Belt, b) Pieninicum; 14 – Inner Carpathian Paleogene; 15 – Inner Carpathian Mesozoic (envelope series – Krížna, Choč and higher Nappes); 16 – Tatric crystalline schists; 17 – Tatric granitoids; 18 – Crataceous intrusive rocks (a – granites, b – granitoids); 19 – Veporic crystalline schists, 20 – Veporic granitoids; 21 – Neogene intrusive rocks (a – diorites, b – gabbrodiorites, gabbros); 22 – Gemeric Paleozoic; 23 – Paleozoic and crystalline rocks of unknown assignation; 24 – basalts; 25 – Neogene cover; 26 thrust lines; 27 – faults (a – crustal, b – deep-seated); 28 – rock density in Mgm^{-3}.

I–IX – see legend to Fig. 6 (profile KP-II).

Density models

Sedimentary rocks of the Neogene Carpathian Foredeep, whose density changes with depth from 2.00 to 2.67 Mgm^{-3}, are of fairly small thickness. In all profiles they gradually deepen beneath units of the Outer Flysch Zone where they pinch out. In the north-western (northern) Western Carpathians, they are underlain by Paleozoic and crystalline rocks of the Bohemian Massif and its cover (East European Platform with its cover). Their thickness ranges from 4 to 10 *km*.

The Carpathian Foredeep is overlain by the Outer Flysch Zone nappes. The total thickness of the latter increases towards the Klippen Belt where it attains 10–12 *km*. Roots of the flysch nappes supposedly extend beneath the Klippen Belt and northern tracts of the Inner Carpathian units.

The Klippen Belt has been regarded as steeply-dipping, almost vertical. At depths of 5–10 *km* it bends beneath the Inner Carpathian units.

As far as the Earth's crust deep structure is concerned, the Western Carpathian Mesozoic yields no significant density contrasts. This is probably caused by small thickness (on average 4 *km*) of the Mesozoic complex as well as by their density which does not substantially differ from the reference model (in general, Mesozoic rock density is similar to the density of the upper crust).

In contrast, granitoid rocks (2.67–2.68 Mgm^{-3}) and crystalline schists of the Tatricum and partly also Veporicum (2.70–2.72 Mgm^{-3}) represent distinct density contrast in the Western Carpathian Earth's crust. Their gravity effects make up a substantial part of the broad gravity low marked by curve G_2 (KP-II, KP-III, KP-IV).

The obtained results suggest that the Western Carpathian gravity low reflects combined gravity effects of sedimentary rocks in the Carpathian Foredeep as well as flysch nappes on one side, and Tatric and partly also Veporic granitoid rocks along with crystalline schists on the other side. Gravity effects of the Tatricum and Veporicum are evident particularly in central tracts of the profiles.

Fig. 6 Density and geothermal model of Earth's crust in profile KP-IV.

Legend: 1 – boundaries of principal geological units (A – Platform, B – Flysch Belt, C – Klippen Belt, D – Inner Carpathian Paleogene, E – Inner Carpathian Mesozoic, F – Tatricum, G – Veporicum, H – Neogene; 2–7 – see explanations to Fig 4; 8 – lower crust; 9 – lower part of upper crust; 10 – Bohemian Massif and Platform crystalline and Paleozoic, 11 – Foredeep; 12 – Flysch Belt (a – Silesian Nappe, b – Magura Nappe); 13 – Klippen Belt; 14 – Inner Carpathian Paleogene; 15 – Inner Carpathian Mesozoic (envelope nappe – Krížna, Choč and higher Nappes); 16 – Tatric crystalline schists; 17 – Tatric granitoids; 18 – Neogene intrusive rocks (a – diorites, b – gabbrodiorites, gabbros); 19 – neovolcanic rocks; 20 – Veporic granitoids; 21 – Veporic crystalline schists; 22 – granite intrusives; 23 – Gemeric Paleozoic; 24 – Paleozoic and crystalline rocks of unknown assignation; 25 – basalts; 26 – Neogene cover; 27 – thrust lines; 28 – faults (a – crustal, b – deep-seated); 29 – rocks density in Mgm^{-3}.

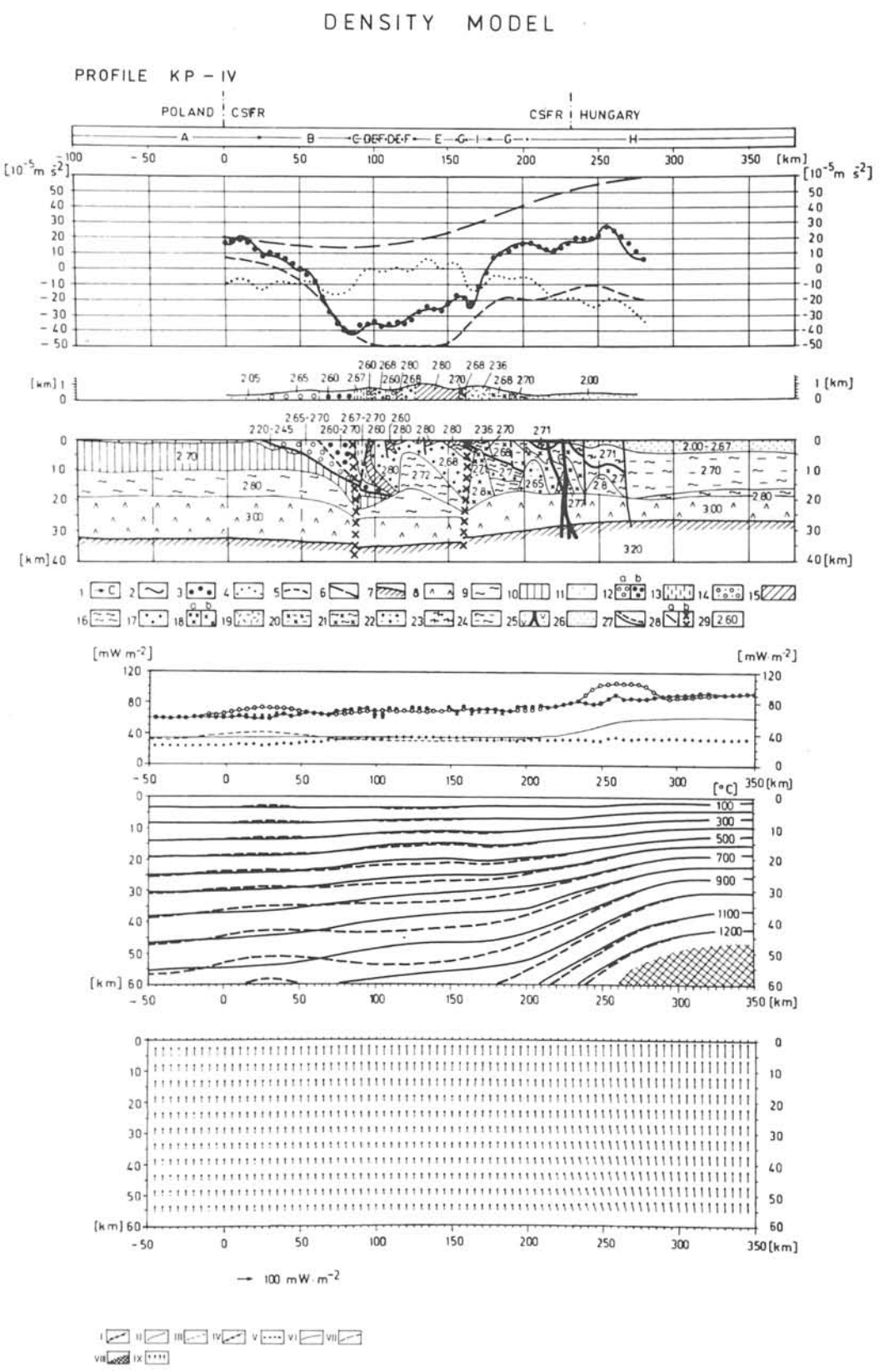

I – surface heat flow (=HF) values inferred from maps; II – HF values at lower boundary of profile for basic model; III – HF values at lower boundary calculated by resolving inverse problem; IV – calculated values of surface HF; V – surface HF values of radiogenic origin; VI – thermal field pattern in profile of basic model; VII – thermal field pattern after resolving inverse problem; VIII – area of possible partial melting in upper mantle; IX – HF pattern in profile section (profile KP-II).

In the Veporic area, we have interpreted young crustal abyssal bodies (Rochovce, Central Slovakian Neovolcanics). At shallower parts of the upper Earth's crust there occur bodies of granitoid character (granites, granodiorites and diorites – KP-II, KP-III, KP-IV). Their density, however, supposedly increases with depth (where the rocks comprise mainly granodiorites, gabbrodiorites and gabbros), as can be seen on profiles KP-III and KP-IV.

The used average differential density of the Gemeric Paleozoic is not very high, although Husák's (1986) investigations suggest that the Early Paleozoic rock densities are more contrast. In addition, its gravity effect is probably compensated by a low-density granitoid body whose apical parts are exposed on the surface in several places of this area.

The lower crust, whose average density has been estimated at 3.00–3.10 Mgm^{-3}, is 8–14 *km* thick in Inner Carpathians and Pannonian Basin, and its thickness increases towards the Bohemian Massif and East European Platform.

The depth of the Moho discontinuity increases from some 26 *km* in the Pannonian Basin to 32–36 *km* in the Outer Western Carpathian margin.

Geothermal models

The results obtained as well as the basic map of surface heat flow density pattern indicate that temperature and heat flow density in the Western Carpathians reflect complexity of their structure and history. From a regional point of view, the geothermal activity drops from the Western Carpathian Inner units towards the outer ones. The geothermal modelling confirmed, however, that this decline in heat flow density and temperature pattern is neither even nor regular. According to the thermal activity, the Western Carpathians can be divided into two parts. One of them, on average less active, comprises the Outer Carpathians along with northern and central parts of the Inner Carpathians. The other part, characterized by high activity, consists of the neovolcanic belt and Inner Carpathian Neogene basins (except for the Vienna Basin). Heat transfer from the mantle gives rise to heat flow densities ranging from 25 to 65 mWm^{-2} the highest heat flow densities probably occurring at the Pannonian Basin margin. The lowest values are in the Western Carpathian outer units north of the Vysoké Tatry Mts. Temperatures at the Moho discontinuity fall from 900 to 400 °*C*.

The analysis of the mutual relationship suggests that surface heat flow density declines with increasing Earth's crust thickness in the predominant part of the Western Carpathians (except for the neovolcanic region and considerably hydrogeologically affected areas). Regions with a thin Earth's crust are characterized by increased values of surface heat flow density and vice versa.

Furthermore, calculations along profiles KP indicate that heat flow density from radiogenic crustal sources in the Bohemian Massif, Platform and Western Carpathian outer units accounts for 40-50 % of the total surface heat flow density. In the Inner Carpathians their share is over 50 %. This is due to larger accumulation of masses with higher heat generation because of the nappe structure of the region. The maximum effects of such radiogenic sources have been observed in the Gemeric area where highly radioactive Paleozoic rock complexes and Gemeric granites are concentrated. The share of crustal radiogenic heat sources in the surface heat flow density declines towards the Pannonian Basin to 30–40 %. This smaller share of crustal radiogenic heat sources can be explained by thin crust but mainly high heat flow density from the mantle.

Higher absolute values and variability of heat generation as well as irregular distribution of thermal conductivity coefficient are reflected by higher inhomogeneity in observed heat flow density and temperature distribution on regional background (e.g. granites, poorly conductive rock intercalations in the Gemeric Paleozoic, northern margins of the Pannonian Basin etc.). This inhomogeneity, however, is also caused by some other phenomena – hydrogeological conditions (e.g. in intermontane basins), cooling volcanic rocks (Central Slovakian Neovolcanics, Matra Mts. etc.), age of the last thermal activation, deposition, denudation, nappe overthrusting, carbonization and of course combined effects of several phenomena (e.g. Ostrava Basin, Miskolc area). Profiles KP-II to KP-IV described in this article are situated in the area which was fairly poorly thermally investigated. To increase the accuracy of the presented models, further measurements of surface heat flow density are necessary.

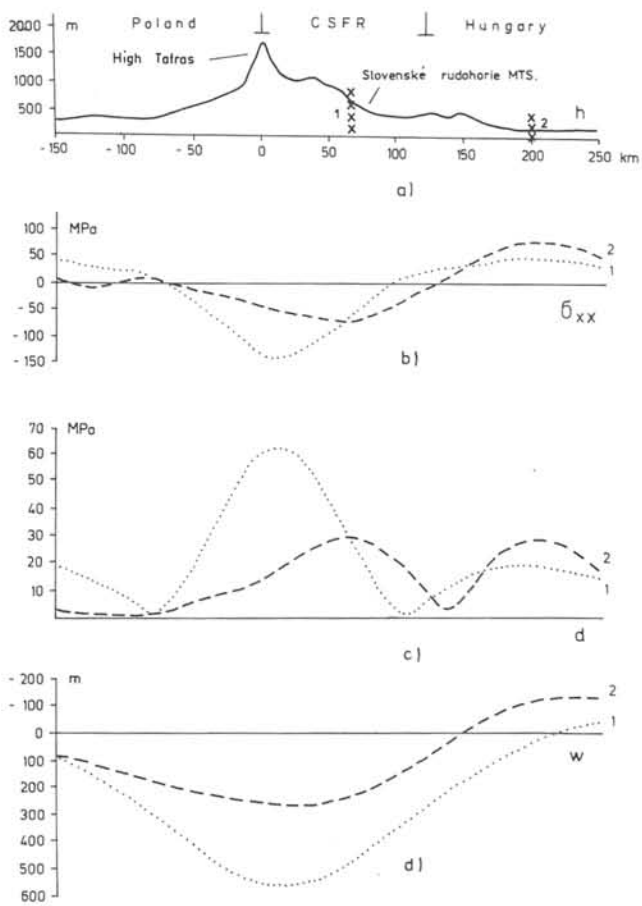

Fig. 7. Stress and displacement fields in profile KP-III.
a – topographic section, 1 – deep-seated Vepor fault (after Fusán et al. 1987); 2 – Balaton fault line (after Fülöp et al. 1987); **b** – course of horizontal stress, 1 – topographic effect, 2 – effects of topography and internal density inhomogeneities; **c** – course of deviation stress, 1, 2 – same as in case b; **d** – course of vertical lithospheric bend, 1, 2 – same as in cases b and c.

Stress fied

Stress fields were calculated along profile KP-III (total length 400 *km*). The following parameters were determined: elasticity coefficient $\mu = 30$ *GPa*, elastic slab thickness $H = 30$ *km*, number of layers $n = 6$ and densities were equal to those in the reference model. Crustal density inhomogeneities (taken from density model of KP-III) in the individual layers were generalized as is shown in Fig. 3. The first variant of the calculation assumed separate effect of terrain topography, whereas the other one was based on combined effects of topography and internal density inhomogeneities. The results of the calculations are given in Fig. 7a – 7c.

The predominant component is horizontal stress σ_{xx} (Fig. 7a). If we take into account only the effect of topography, compressive horizontal stress attains its highest value of 140 *MPa* in the Vysoké Tatry area, whereas in the Hungarian territory there occur tensile stresses of 42 *MPa*. Owing to subcrustal inhomogeneities, the maximum compressive stress falls to 72 *MPa* and moves into the Vepor fault area. In contrast, gravity stress increases to 74 *MPa* in the Balaton fault line area.

Fig. 7b shows the course of magnitude of deviation stress calculated according to the formula

$$d = \sqrt{1/4\,(\sigma_{xx} - \sigma_{zz})^2 + \sigma_{xz}^2}\ .$$

The amplitudes of deviation stress attain 30 *MPa* in the Slovenské rudohorie Mts. and Balaton fault line area.

The course of the vertical bend of the elastic slab lower boundary is illustrated in Fig. 7c. The band caused by topographic relief alone amounts to 570 *m* in the Vysoké Tatry area. Crustal inhomogeneities, however, reduce this maximum value to 270 *m* and displace it moderately in the horizontal direction. On the contrary, in the Pannonian Basin area it was uplifted by as much as 140 *m*. The above-mentioned results suggest that the stress field generated by terrain topography may be considerably modified due to internal density inhomogeneities.

Translated By Ľ. Böhmer

References

Biela A., 1978: Hlboké vrty v zakrytých oblastiach vnútorných Západných Karpát I., II. Regionálna geológia Západných Karpát. *GÚDŠ*, Bratislava, 1–224.

Bielik M., Budra M., Vyskočil V. & Hübner M., 1987: Nové varianty hustotných modelov pozdĺž profilov HSS. In: *Problémy současné gravimetrie. GFÚ ČSAV* Praha – *Geofyzika* Brno, 9–15.

Blížkovský M., Burda M., Ibrmajer J., Jakubcová J., Pick M., Suk M. Vyskočil V., 1985: Modelling of the density distribution of the Bohemian Massif. *Internat. Workshop* – ETH Zürich, 28–31.

Blížkovský M. et al., 1986: Geofyzikální model litosféry. Závěreční zpráva úkolů OTFR – ČGÚ č. 82–160 za období 1982–1985. GFÚ ČSAV Praha – Geofyzika Brno, š. p. Bratislava, GFÚ SAV, 1–424.

Bott M. H. P. & Kusznir N. J., 1984: The origin of tectonic stress in the lithosphere. *Tectonophysics*, 105, 1–3.

Burda M., Hübner M., Vyskočil N., Blížkovský M., Novotný A., Suk M., Bielik M. & Fusán O., 1985: Hustotní model litosféry pro čs. úsek geotraverzy č. V. In: *Problémy současné gravimetrie. GFÚ ČSAV* Praha – *Geofyzika* Brno, 297–308.

Büntebarth G., 1982: Density and seismic velocity in relation to mineralogical constitution based on an ionic model for minerals. *Earth Planet. Sci. Lett.*, 57, 358–366.

Čermák V. & Bodri L., 1985: Temperature structure of the lithosphere based on 2-D temperature. Modelling applied to Central and Eastern Europe. In: *Thermal modelling in sedimentary basins. Technip*, 17–42.

Eliáš M. & Uhmann J., 1968: Hustoty hornín ČSSR. Vysvětlivky k mapě hustot hornin ČSSR 1 : 500 000. *ÚÚG*, Praha, 1–44.

Eringen A. C., 1967: Mechanics of continus. *Wiley*, New York, 1–210.

Fusán O. et al., 1987: Podložie terciéru vnútorných Západných Karpát. *GÚDŠ*, Bratislava, 1–123.

Fülöp J. et al., 1987: Precenozoic basement map of Hungary 1: 500 000. *Hung. Geol. Inst.*, Budapest.

Husák L., 1986: Hustota a rádioaktivita hornín vnútorných Západných Karpát. Dielčia záverečná správa. Manuscript, Geogond, Bratislava.

Ibrmajer J., 1978: Tíhové mapy ČSSR a jejich geologická interpretace. *Fac. of Sci., Charles Univ.*, Praha, 1–240.

Král M., 1987: Heat flow map of the West Carpathians. Manuscript, Geofyzika, Brno.

Král M., Lizoň I. & Jančí J., 1985: Geotermický výskum SSR. Záverečná správa. Manuscript, Geogond, Bratislava.

Majcin D., 1989: Geotermický model Západných Karpát. Thesis, GFÚ CGF SAV, Bratislava, 1–136.

Mayerová M. et al., 1985: Plošné rozložení Moho-plochy v ČSSR sestavené z výsledků profilových měření HSS a technických odpalů. *8. celostátní konference geofyziků. Sekce S1 – seizmická.* Geofyzika, Brno, 44–53.

Rasmussen R. & Federsen L. B., 1979: End correction in potential field modelling. *Geophysical Prospecting*, 27, 749–760.

Rybach L. & Büntebarth G., 1982: Relationships between the petrophysical properties density, seismic velocity, heat generation and mineralogical constitution. *Earth Planet. Sci. Lett.*, 57, 367–376.

Rybach L. & Büntebarth G., 1984: The variation of the heat generation, density and seismic velocity with rock type in the continental lithosphere. *Tectonophysics*, 103, 335–334.

Samarsky A. A. & Nikolayev E. C., 1978: Metodi resheniya setochnikh uravneniy. *Nauka*, Moskva, 1–589.

Samarsky A.A. & Andreyev V. B., 1976: Raznostaniye metodi dlya ellipticheskikh uravneniy. *Nauka*, Moskva, 1–286.

Šefara J. et al., 1987: Štruktúrno-tektonická mapa vnútorných Západných Karpát pre účely prognózovania ložísk – geofyzikálne interpretácie. SGÚ Bratislava – Geofyzika Brno. UP, K. P. Liberec, 1–267.

Talwani M., 1973: Computer usage in the computation of gravity anomalies. In: *Methods in computational physics*, 13, 343–389.

Tomek Č., Dvořáková L., Ibrmajer I., Jiříček R.&Koráb T., 1987: Crustal profiles of active contintal collisional belt: Czechoslovak deep seismic reflection profiling in the West Carpathians. *Geophys. J. R. Astr. Soc.*, 89, 383–388.

Tomek Č., Ibrmajer I., Koráb T., Biely A., Dvořáková L., Lexa J. & Zbořil A., 1989: Crustal structure of the West Carpathians on deep reflection seismic line 2T. *Mineralia slov.* (Košice), 21, 2–26.

Turcotte D. L. & Oxburgh E. R., 1976: Stress accumulation in the lithosphere. *Tectonophysics*, 35, 183–199.

Turcotte D. L. & Schubert G., 1982: *Geodynamics. Wiley*, New York, 1–730.

Vazov V. R. & Forsyt G. E., 1963: Raznostniye metodi dlya uravneniy v chastnikh proizvodnikh. *Izv. Inostr. lit.*, Moskva, 1–486.

Vyskočil V., Burda M., Bielik M.& Fusán O., 1990: Ďalšie hustotné modely Západných Karpát. *Contrib. Geophys. Inst. Slov. Acad. Sci.* (Bratislava).

Watts A. B., Cohran J. R. & Selzer G., 1975: Gravity anomalies and flexure of the lithosphere: A three-dimensional study of the Great Meteor Samount, Northeast Atlantic. *J. Geophys. Res.*, 80, 1391–1398.